View metadata, citation and similar papers at core.ac.uk
brought to you by CORE
provided by Archivio della Ricerca - Università di Pisa

PHYSICAL REVIEW D **91,** 035006 (2015)

Leptoquarks, dark matter, and anomalous LHC events

Farinaldo S. Queiroz,[1,*] Kuver Sinha,[2,†] and Alessandro Strumia[3,4,‡]

[1]*Department of Physics and Santa Cruz Institute for Particle, Physics University of California, Santa Cruz, California 95064, USA*
[2]*Department of Physics, Syracuse University, Syracuse, New York 13244, USA*
[3]*Dipartimento di Fisica dell' Universita di Pisa and INFN, Tuscany, Pisa, Italy*
[4]*National Institute of Chemical Physics and Biophysics, Tallinn, Estonia*

(Received 8 November 2014; published 5 February 2015)

Leptoquarks with mass in the region of 550–650 GeV are a possible candidate for the recent excess seen by CMS in the $eejj$ and $e\nu jj$ channels. We discuss models where leptoquarks decay primarily to dark matter and jets, thereby giving a branching to charged lepton and jet final states that can match data. The confluence of proton decay constraints, dark matter indirect and direct detection data, and Higgs invisible decay bounds results in a handful of predictive models that will be conclusively verified or excluded in upcoming direct detection experiments. Along the way, we present robust limits on such leptoquark models stemming from the muon magnetic moment using current and projected experiment sensitivities, as well as from K and B meson mixing, and leptonic and semileptonic meson decays.

DOI: 10.1103/PhysRevD.91.035006 PACS numbers: 95.35.+d, 12.60.Cn, 12.60.Fr, 95.30.Cq

I. INTRODUCTION

Leptoquarks (LQs) are bosons that couple to a quark and a lepton. While not essential elements in addressing today's most outstanding questions (such as the gauge hierarchy problem or the identity dark matter), these particles have a venerable history in particle physics, going back at least to the Pati-Salam model [1], $SU(5)$ grand unification [2], and technicolor [3].[1]

LQs are strongly interacting, and their decay products include leptons. This fact alone makes them promising search candidates at hadron colliders; indeed, both CMS and ATLAS have placed stringent limits on their masses.

For second-generation LQs, CMS has performed searches with 19.6 fb^{-1} of data focusing on the $\mu\mu jj$ and $\mu\nu jj$ final states, which have resulted in the exclusion of scalar LQs with masses below 1070 (785) GeV for $\mathrm{Br}_{\mu j} = 1(0.5)$ [8,9]. Similarly, third-generation scalar LQs with masses below 740 GeV are excluded at 95% C.L., assuming 100% branching fraction for the LQ decay to a τ lepton and a bottom quark [10], whereas the case of branching ratio of 100% into top quark-τ lepton pairs is ruled out up to a mass of 634 GeV [11].

Searches for the first generation of letptoquarks, on the other hand, have resulted in mild evidence for ~650 GeV scalar LQs. The CMS Collaboration using 19.6 fb^{-1} of integrated luminosity has revealed a 2.4σ and 2.6σ excess in the $eejj$ and $e\nu jj$ channels, respectively, after optimizing cuts for a 650 GeV LQ [12].

An interesting feature of the recent excess seen in the first-generation searches is that the branching into lepton and jets final states cannot be the entire story. LQs are produced dominantly through gluon fusion and quark-antiquark annihilation. The NLO production cross section for a 650 (550) GeV LQ is 0.0132 (0.0431) pb, with a PDF uncertainty of 0.00322 (0.00893) pb. If the renormalization/factorization scale is varied between half the LQ mass and double the LQ mass, the cross sections are 0.0113 (0.037) pb and 0.0149 (0.0485) pb, respectively. On the other hand, the observed cross section times the branching to lepton and jets final states is much smaller than the theoretical prediction. In fact, a recent study [13] of the excess has concluded that for a 550 GeV LQ, the best fits are obtained for $\mathrm{Br}_{ej} = 0.12$ and $\mathrm{Br}_{\nu j} = 0.15$, while for a 650 GeV LQ, the branching ratios are $\mathrm{Br}_{ej} = 0.21$ and $\mathrm{Br}_{\nu j} = 0.13$. In other words, there is a significant branching of LQs into other states, potentially dark matter.

The excess observed is clearly preliminary, and results from the 14 TeV run should be watched carefully. Nevertheless, it is worthwhile to explore model building possibilities in case the signal does hold up. A theoretically appealing scenario would arise if LQs are tied to dark matter while obeying current constraints.

The purpose of this paper is to outline possible scenarios that fulfill these criteria. In particular, we study frameworks where a 550–650 GeV LQ possibly has significant branching to dark matter, and present the confluence of proton decay constraints, indirect and direct dark matter detection bounds and the Higgs invisible decay limits in such a setting. This turns out to be remarkably predictive and verifiable, and for the benefit of the reader, we summarize our results here.

*fdasilva@ucsc.edu
†kusinha@syr.edu
‡Alessandro.Strumia@cern.ch

[1]We refer to [4–6] and references therein for more of the early literature. LQs also appear in a variety of other contexts, of which we cite a few examples [7].

 © 2015 American Physical Society

Proton decay constraints limit the possible scalar LQ models to just two—those where the LQs are doublets under $SU(2)$. The LQ gauge charges pick out the following dark matter candidates (after requiring dark matter stability): (i) scalar or fermionic triplets, which are ruled out by Fermi-LAT data in the mass range of interest and (ii) scalar or fermionic singlets, which are within reach of the projected XENON1T experiment in the mass range of interest.

Along the way, we present robust limits stemming from the muon magnetic moment using current and projected experiment sensitivities, as well as coming from K and B meson mixing, and leptonic and semileptonic meson decays.

The paper is organized as follows. In Sec. II, we write down the possible LQ models and discuss relevant proton decay, muon magnetic moment, and meson mixing and decays bounds. In Sec. III, we write down our model connecting the LQ and dark matter sectors, whereas in Sec. IV we work out the dark matter phenomenology. Lastly, we end with our conclusions.

II. GENERAL LEPTOQUARK MODELS

In this section, we first present simplified models of scalar LQs and discuss stringent bounds stemming from the muon magnetic moment, collider, flavor and proton decay bounds. A general classification of renormalizable LQ models can be found in [14,15]. The relevant models, following the notation of Ref. [14], are listed in Table I. For reasons that will be clear later, we will be mostly interested in the models containing R_2 and $\tilde{R}_2$, where the latter will be our primary focus when we discuss the dark matter phenomenology and the connection to the recent CMS excess. The model containing $\tilde{R}_2$ has a Lagrangian given by

$$\mathcal{L} = -\lambda_d^{ij}\bar{d}_R^i \tilde{R}_2^T \epsilon L_L^j + \text{H.c.}, \tag{1}$$

where (i, j) denote flavor indices. Expanding the $SU(2)$ indices yields

$$\mathcal{L} = -\lambda_d^{ij}\bar{d}_{\alpha R}^i (V_\alpha e_L^j - Y_\alpha \nu_L^j) + \text{H.c.} \tag{2}$$

TABLE I. Interaction terms for scalar LQs allowed by symmetries. Note that all the LQ candidates have $L = -1, B = 1/3$, $B - L = 4/3$.

Leptoquark notation	Leptoquark couplings	$SU(3) \times SU(2) \times U(1)$ representation of LQ
R_2	$R_2\bar{Q}e$, $R_2 L\bar{u}$	$(3, 2, 7/6)$
$\tilde{R}_2$	$\tilde{R}_2 L\bar{d}$	$(3, 2, 1/6)$
S_1	$S_1\bar{Q}\,\bar{L}$, $S_1\bar{u}\,\bar{e}$	$(3, 1, -1/3)$
S_3	$S_3\bar{Q}\,\bar{L}$	$(3, 3, -1/3)$
$\tilde{S}_1$	$\tilde{S}_1\bar{d}\,\bar{e}$	$(3, 1, -4/3)$

Similarly, the model containing R_2 has the following Lagrangian:

$$\mathcal{L} = -\lambda_u^{ij}\bar{u}_R^i R_2^T \epsilon L_L^j - \lambda_e^{ij}\bar{e}_R^i R_2^\dagger Q_L^j + \text{H.c.}, \tag{3}$$

where

$$R_2 = \begin{pmatrix} V_\alpha \\ Y_\alpha \end{pmatrix}, \qquad \epsilon = \begin{pmatrix} 0 & 1 \\ -1 & 0 \end{pmatrix}, \qquad L_L = \begin{pmatrix} \nu_L \\ e_L \end{pmatrix}. \tag{4}$$

After expanding the $SU(2)$ indices it takes the form

$$\mathcal{L} = -\lambda_u^{ij}\bar{u}_{\alpha R}^i (V_\alpha e_L^j - Y_\alpha \nu_L^j) - \lambda_e^{ij}\bar{e}_R^i (V_\alpha^\dagger u_{\alpha L}^j + Y_\alpha^\dagger d_{\alpha L}^j) + \text{H.c.}, \tag{5}$$

where the same notation as before has been used. Now we will turn our attention to discussing important bounds on LQs.

A. Proton decay

A very important issue to be accounted for in LQ models is baryon number violation, due to the strong bounds on processes like $p \to \pi^0 e^+$. Only those models that have no proton decay in perturbation theory should be considered. Hence the fields S_1, S_3, and $\tilde{S}_1$ that allow the respective operators $S_1 QQ + S_1 ud, S_3 QQ$, and $\tilde{S}_1 uu$ are ignored since they induce fast proton decay via tree-level scalar LQ exchange. For the LQs, R_2 and $\tilde{R}_2$, symmetries disallow couplings of these operators to quark bilinears; hence, there is no proton decay diagram via LQ exchange at dimension four [16]. However, there are still dangerous dimension-five operators, namely,

$$\mathcal{L}(R_2) \supset \frac{1}{\Lambda} g^{ab} d_{R\alpha}^a d_{R\beta}^b (H^\dagger R_{2\gamma}) \epsilon^{\alpha\beta\gamma} \tag{6}$$

$$\mathcal{L}(\tilde{R}_2) \supset \frac{1}{\Lambda} g^{ab} u_{R\alpha}^a d_{R\beta}^b (H^\dagger \tilde{R}_{2\gamma}) \epsilon^{\alpha\beta\gamma} \tag{7}$$

$$\mathcal{L}(\tilde{R}_2) \supset \frac{1}{\Lambda} g^{ab} u_{R\alpha}^a e_R^b (\tilde{R}_{2\beta} \epsilon \tilde{R}_{2\gamma}) \epsilon^{\alpha\beta\gamma}. \tag{8}$$

For example, in Fig. 1 we display a diagram that shows baryon number violating decay involving the LQ R_2. We stress that the coupling constant matrix g is antisymmetric in flavor space. Note that Eq. (6) leads to the nucleon decay $n \to e^- K^+$ and $p \to K^+ \nu$, whereas Eq. (7) induces $n \to e^- \pi^+$ and $p \to \pi^+ \nu$. The lifetime of such decays is short, demanding that the LQs masses lie much above the TeV scale.

A simple way to prevent these operators is to impose a Z_3 symmetry under which fields carry charges $\exp[2\pi i(B - L)/3]$ [16]. It is easy to check that imposing

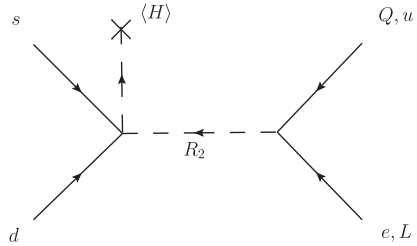

FIG. 1. Diagram for proton decay.

this symmetry (or any other discrete subgroup of $U(1)_{B-L}$) will not remedy the tree-level proton decay induced by the LQs S_1, S_3, and $\tilde{S}_1$, since all the relevant interactions in those cases conserve $B-L$. In conclusion, in order to have a plausible LQ model with proton stability, LQs that are doublets under $SU(2)$ are preferred, and moreover some sort of discrete symmetry must be invoked. Particularly, in the case of LQs R_2 and $\tilde{R}_2$, it is a Z_3 one.

B. Muon magnetic moment

The muon magnetic moment is one of the most precisely measured quantities in particle physics, and a 3.6σ discrepancy has been observed recently indicating that new physics may be around the corner. Despite the uncertainties rising from hadronic contributions, the current deviation is reported as $\Delta a_\mu = (295 \pm 81) \times 10^{-11}$ [17]. The combined effort from the theoretical and experimental side expects to reduce the uncertainties down to $\Delta a_\mu = (295 \pm 34) \times 10^{-11}$ [17]. The latter is referred as our projected bound. In this context, through the diagrams shown in Fig. 2, LQs give rise to sizeable contributions according to Eq. (9) [17],

$$\Delta a_\mu(V) = \frac{1}{8\pi^2}\frac{N_c Q_q m_\mu^2}{M_V^2}\int_0^1 dx \frac{g_s^2 P_s(x) + g_p^2 P_p(x)}{(1-x)(1-\lambda^2 x) + \epsilon^2\lambda^2 x} + \frac{1}{8\pi^2}\frac{N_c Q_\Phi m_\mu^2}{M_\Phi^2}\int_0^1 dx \frac{g_s^2 P'_s(x) + g_p^2 P'_p(x)}{\epsilon^2\lambda^2(1-x)(1-\epsilon^{-2}x) + x}, \tag{9}$$

where $\epsilon = m_q/m_\mu$ and $\lambda = m_\mu/M_V$, $m_q(Q_q)$ is the mass (electric charge) of the quark running in the loop, g_s and g_a are the respective scale and pseudoscalar couplings to muons, and

$$\begin{aligned} P'_s(x) &= x^2(1+\epsilon-x), \\ P'_p(x) &= x^2(1+\epsilon-x), \\ P'_s(x) &= -x(1-x)(x+\epsilon), \\ P'_p(x) &= -x(1-x)(x-\epsilon). \end{aligned} \tag{10}$$

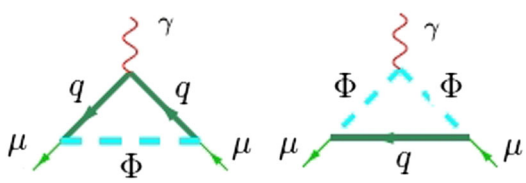

FIG. 2 (color online). Diagrams involving general LQs (Φ) that contribute to muon $g-2$.

In Fig. 3 we show contributions to the muon magnetic moment for the LQ R_2 with couplings of order one. The green solid (dashed) horizontal lines are the current and projected Δa_μ. The red ones are the current (projected) 1σ limits assuming the anomaly is otherwise resolved. One can clearly notice that the quark mass running in the loop is important to the overall correction to g-2 since the different generations yield different results. The contributions to the muon magnetic moment are negative for all generations.

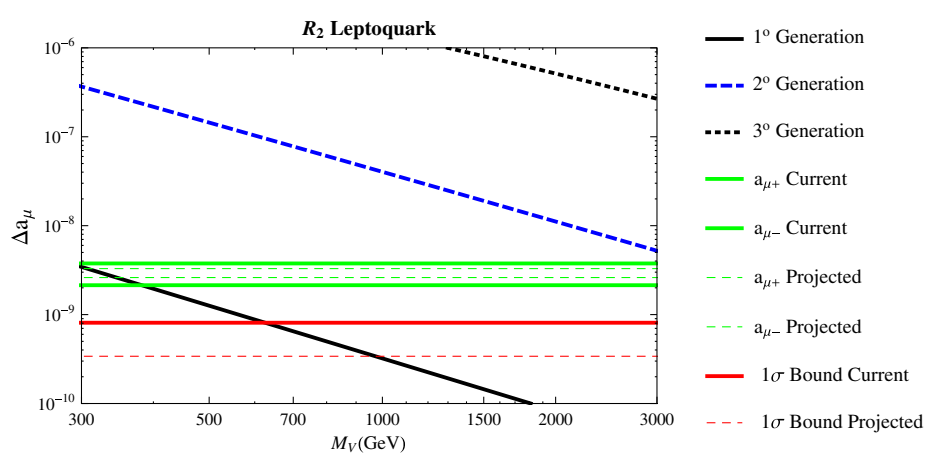

FIG. 3 (color online). Contributions to the muon magnetic moment coming from first-, second-, and third-generation leptoquarks R_2 for unity leptoquark couplings. All individual contributions scale as the square of the couplings and are negative. We plotted the absolute value of the contributions compared to current measurements. The green solid (dashed) horizontal lines are the current and projected Δa_μ. The red ones are the current (projected) 1σ limits assuming the anomaly is otherwise resolved.

TABLE II. Limits on the couplings for the leptoquark models of interest. We emphasize that the corrections to g-2 rising from all these models are negative, and therefore they cannot accommodate the muon magnetic moment deviation, but 1σ bounds can still be placed under the assumption the anomaly is otherwise resolved. The overall $\tilde{R}_2$ contribution is quite small and, hence, no meaningful limit could be placed.

Model	Limit
g-2 bounds on 650 GeV leptoquarks	
R_2: 1° generation	coupling < 1
R_2: 2° generation	coupling < 0.1
R_2: 3° generation	coupling < 0.01
$\tilde{R}_2$: 1°, 2°, 3° generation	No bound

In any case, we can still place limits on the masses of the LQs since their contributions have to be within the 1σ error bars. That being said, we derive the following limits: $M_V >$ 600 GeV (first generation), $M_V > 8$ TeV (second generation), and $M_V > 50$ TeV (third generation). We point out that our limits are valid for couplings of order one. Since $\Delta a_\mu \propto \text{coupling}^2$ the limits are strongly sensitive to the couplings' strength.

Focusing on 650 GeV R_2, we find the following constraints on couplings: $\lambda \leq 1$ (first generation), $\lambda \leq 0.1$ (second generation), and $\lambda \leq 0.01$ (third generation), where $\lambda' s$ refer to the muon-leptoquark couplings. A summary of those limits is presented in Table II. In conclusion, we emphasize that a first-generation 650 GeV R_2 LQ is not ruled out by g-2 and it is, in principle, a suitable candidate to explain the CMS excess.

As for the $\tilde{R}_2$ LQ, the overall corrections to g-2 are negative and small enough so that no meaningful limit can be placed either on the couplings or the masses. Thus, $\tilde{R}_2$ 650 GeV leptoquarks are also viable candidates to the explain the CMS excess.

C. K and B physics constraints

Scalar LQs such as the ones presented in Eq. (1) contribute to the K and B meson mixing, as well as leptonic and semileptonic meson decays from those mesons. Therefore, using current data important constraints might be derived. We refer to Ref. [18] for limits on various LQs models. Here we are focused on the LQ $\tilde{R}_2$ because it the relevant one for our further discussions. In this context of mesons mixing, meson oscillations $M^0 - \overline{M^0}$ can have a new LQ mediated amplitude, with i-type leptons and some scalar LQ. The amplitude is proportional to $(\lambda_{ik}\lambda_i)^2$, that rises from the effective operator $[\bar{b}\gamma_\mu P_R d][\bar{d}\gamma_\mu P_R b]$. As for the leptonic $(B^0_{d,s} \to l^+l^-, K^0 \to l^+l^-)$ and semileptonic $(b \to dl^+l^-, s \to dl^+l^-)$ decays, they are also sensitive to the aforementioned product of couplings. For the LQ $\tilde{R}_2$, the relevant interactions are the four-fermion operators $G(\bar{d}_R\nu_L)(\bar{\nu}_L d_R)$ and $G(\bar{d}_R e_L)(\bar{e}_L d_R)$, where $G \sim \lambda^2/m^2_{LQ}$. In Tables II–IV, we summarize the updated the bounds on the product of lambdas for a 650 GeV LQ following the recipe of Ref. [18]. In the first column of Tables II–V we exhibit bounds on a variety of coupling products. The second and third columns are the bounds on the real and imaginary component of the products rising from the mixing study. In the third column we show which decay channel has been studied; whereas, in the fourth we show the respective constraint. Notice that these limits are complementary to the muon magnetic moment one, but are mostly sensitive to the nondiagonal couplings. We can conclude that order of one diagonal couplings are consistent with data as long as suppressed nondiagonal couplings are used. In other words, a 550–650 GeV LQ might address the muon magnetic moment while being consistent with K and B physics limits. After discussing proton decay, muon magnetic moment and electroweak constraints, we summarize in the next section the collider bounds.

D. Collider bounds

After LQs are pair produced through QCD interactions, they decay to final states containing jets and leptons. The bounds on the LQ masses thus depend on the branching fraction to the various channels. Searches have been conducted for all the generations. CMS has studied first-generation LQs with 19.6 fb^{-1} of data at the 8 TeV LHC. Events with $eejj$ and $e\nu jj$ final states have been targeted. For the $eejj$ channel, events with exactly two electrons with $p_T > 45$ GeV, and at least two jets with $p_T > (120, 45)$ GeV have been selected; subsequently, for

TABLE III. Bounds coming from $K^0 - \bar{K}^0$ mixing and correlated decays.

	Bounds			
	From mixing		From decay	
Yukawa $\lambda_{(..)}\lambda^*_{(..)}$	Real part	Imag. part	Channel	Bound
$(11)(12)^*$	1.2×10^{-3}	1.2×10^{-3}	$K^+ \to \pi^+ e^+ e^-$	2.6×10^{-4}
			$K_L \to \pi^0 e^+ e^-$	6.0×10^{-6}
$(21)(22)^*$	1.2×10^{-3}	1.2×10^{-3}	$K^+ \to \pi^+ \mu^+ \mu^-$	2.0×10^{-4}
			$K_L \to \mu^+ \mu^-$	1.4×10^{-6}
$(31)(32)^*$	1.2×10^{-3}	1.2×10^{-3}	$K_L \to \pi^0 \nu\bar{\nu}$	1.0×10^{-4}

TABLE IV. Bounds coming from $B_d - \bar{B}_d$ mixing and correlated decays.

	Bounds			
	From mixing		From decay	
Yukawa $\lambda_{(..)}\lambda^*_{(..)}$	Real part	Imag. part	Channel	Bound
$(11)(13)^*$	0.03	0.03	$B^+ \to \pi^+ e^+ e^-$	1.1×10^{-4}
$(21)(23)^*$	0.03	0.03	$B^+ \to \pi^+ \mu^+ \mu^-$	1.0×10^{-4}
$(31)(33)^*$	0.03	0.03	$B^+ \to \pi^+ \nu\bar{\nu}$	4.3×10^{-3}

TABLE V. Bounds coming from $B_s - \bar{B}_s$ mixing and correlated decays.

	Bounds			
	From mixing		From decay	
Yukawa $\lambda_{(..)}\lambda^*_{(..)}$	Real part	Imag. part	Channel	Bound
$(12)(13)^*$	0.02	0.02	$B_d \to K^0 e^+ e^-$	7.7×10^{-5}
$(22)(23)^*$	0.02	0.02	$B_d \to K^* \mu^+ \mu^-$	2.3×10^{-4}
$(32)(33)^*$	0.02	0.02	$B^+ \to K^+ \nu\bar{\nu}$	2.0×10^{-3}

different LQ masses, the invariant mass m_{ee} of the electrons, the scalar sum S_T of the p_T of the two leading jets and the two electrons, and the average electron-jet invariant mass m_{ej}, obtained from the two electrons and two jets, were optimized. For the benchmark point of $m = 650$ GeV, the cuts were $m_{ee} > 155$, $S_T > 850$, and $m_{ej} > 360$ GeV. Thirty-six signal events were observed, against an expected background of $20.49 \pm 2.14 \pm 2.45(\mathrm{syst})$, yielding a significance of 2.4σ. Interestingly, the number of signal events is lesser than the expected signal for a LQ decaying purely into electrons and jets with 100% branching ratio. This implies that there is nonzero branching to other states. In the $e\nu jj$ channel, the optimized cuts are $S_\mathrm{T} > 1040$, $E_\mathrm{T}^\mathrm{miss} > 145$, $m_\mathrm{ej} > 555$, and $m_{\mathrm{T},e\nu} > 270$ GeV. Eighteen signal events were observed over a background of $7.54 \pm 1.20 \pm 1.07(\mathrm{syst})$, giving a significance of 2.6. The CMS study cannot exclude LQs with masses of 650 GeV, and branching ratio β to an electron and a quark $\beta < 0.15$. On the other hand, LQs with $\beta = 1(0.5)$ are ruled out up to masses of 950(845) GeV. From the above discussion of bounds, it is clear that if the signal in the $eejj$ and $e\nu jj$ channels are real, LQs have significant branching to other states. Due to the stringent constraints on branching to the second generation, it is natural to consider a scenario where the LQ decays mainly into dark matter. In the next section, we propose models where the latter is fulfilled.

III. LEPTOQUARKS AND DARK MATTER

Given the nature of the signal seen by CMS, it is clear that considering models where the LQ decays primarily to dark matter and jets is well motivated. In this section, we will provide the simplest such models. As we shall see, the confluence of proton decay, dark matter direct and indirect detection bounds, and Higgs invisible decay constraints leads to a few very limited and predictive scenarios.

A. The model

In this work we focus on the LQ $\tilde{R}_2 = (3, 2, 1/6)$, to avoid tree-level proton decay, as described previously. It is natural to connect this field to the left-handed quark doublet. To ensure the stability of the dark matter candidate, we impose a Z_2 symmetry under which the dark sector is odd, whereas the SM + LQ sector is even. In order to have a leptquark connected to dark matter in a gauge-invariant Lagrangian, we need to add at least two fields (S and χ) in the dark sector. Then, to satisfy $SU(2)_L$ charges, an interesting possibility is to also have a gauge singlet scalar S and a color-neutral $SU(2)$ triplet fermion χ. Thus, in addition to the SM, our model has the following content,

$$\tilde{R}_2 = (3, 2, 1/6)_+$$
$$\chi = (1, 3, 0)_- \tag{11}$$

$$S = (1, 1, 0)_-, \tag{12}$$

where we have also displayed the charge under the Z_2. Notice that to conserve lepton number, χ has lepton number $L = 1$. We will require that χ has a Dirac mass term.[2] Several variations of the above model, with different $SU(2)_L$ charge assignments for S and χ, are possible. These options are outlined in Sec. IV C. Here, we will consider mainly the model with the $SU(2)_L$ triplet fermion and singlet scalar. There are no four-dimensional operators connecting the SM + LQ sector to the dark sector (apart from several "Higgs-portal terms" for S, which we will display soon). Up to dimension five, the operators we can write down are the following:

$$L \supset L_{SM} - \lambda_d^{ij} \bar{d}_R^i \tilde{R}_2^T \epsilon L_L^j - \frac{1}{\Lambda_1} h_i S \bar{Q} \chi \tilde{R}_2 - \frac{1}{\Lambda_2} h_i' S \bar{L} \chi H. \tag{13}$$

We have not displayed the kinetic and mass terms for the new fields. The scales Λ_1 and Λ_2 depend on the scale at which new physics sets in (the corresponding effective operators can be realized within renormalizable mediator models), and will be taken to be $\sim$1 TeV.

We now turn to a discussion of the bounds on the Yukawa parameters λ_{ij} in Eq. (13).

[2]We could also accommodate a Majorana mass term if it is generated at a high scale. This will not change our results much.

B. Bounds on Yukawas λ_{ij}

The approximate constraint coming from collider processes is

$$\text{LHC}: \lambda_{ij} \gtrsim 10^{-8}, \tag{14}$$

which comes from ensuring decay at the collision point. This bound is weak enough that it will not affect any of our subsequent analysis. Moreover, the LQ does not couple to the top quark, so there is no m_t enhancement to $\mu \to e\gamma$ due to a charged lepton chirality flip at one loop. Thus, bounds on the Yukawas coming from flavor violation in the charged lepton sector are expected to be small for this model. Much stronger bounds rise from neutral meson mixing and semileptonic and leptonic decays though. These bounds mostly affect off-diagonal entries of the Yukawa matrix as discussed in Sec. II C.

C. Spectrum and decays

It is useful to write

$$\chi = \begin{pmatrix} \frac{1}{\sqrt{2}}\chi^0 & \chi^+ \\ \chi^- & -\frac{1}{\sqrt{2}}\chi^0 \end{pmatrix}. \tag{15}$$

One obtains the same tree-level mass for the neutral and charged eigenstates, while there is a loop-level splitting given by loops of SM gauge bosons. The mass splitting of two states with charges Q and Q' is given by [19]

$$\Delta M = M_Q - M_{Q'} = \frac{\alpha_2 m_\chi}{4\pi}\left\{(Q^2 - Q'^2)s_{\mathrm{W}}^2 f\left(\frac{M_Z}{m_\chi}\right) + (Q - Q')(Q + Q' - 2Y)\left[f\left(\frac{M_W}{m_\chi}\right) - f\left(\frac{M_Z}{m_\chi}\right)\right]\right\}, \tag{16}$$

where

$$f(r) = \begin{cases} +r[2r^3 \ln r - 2r + (r^2-4)^{1/2}(r^2+2)\ln A]/2 \\ -r[2r^3 \ln r - kr + (r^2-4)^{3/2}\ln A]/4 \end{cases}, \tag{17}$$

where the upper and lower results are for a fermion and scalar, respectively, with $A = (r^2 - 2 - r\sqrt{r^2-4})/2$ and s_{W} the sine of the weak angle.

For $m_\chi \sim \mathcal{O}(100-500)$ GeV, one obtains $\Delta M \sim$ 166 MeV.[3] The decay widths of the LQ are given by

$$\Gamma_{\tilde{R}_2 \to (lj)} \simeq \frac{\lambda^2 N_f m_{\tilde{R}_2}}{4\pi} \tag{18}$$

$$\Gamma_{\tilde{R}_2 \to (\chi j)} \simeq \frac{h^2 N_f}{8\pi^2}\frac{m_{\tilde{R}_2}^3}{\Lambda_1^2}, \tag{19}$$

where N_f is the number of colors of the quark in the final state. We have denoted a leptonic final state with l and a quark final state with j. As stated in Ref. [13], an χ^2 fit to the data prefers a 550 GeV LQ with $BR_{\nu j,lj} \simeq 0.15$, or a 650 GeV LQ with $BR_{\nu j} \simeq 0.13$ and $BR_{lj} \simeq 0.21$. Our model is suitable for a 550 GeV LQ since the leptonic branching ratios are the same. We point out that mild changes are expected in the aforementioned meson related bounds in case one targets a 650 GeV LQ. In order to fulfil the former setup, we need $h/\lambda \simeq 5.6$ for $\Lambda = 1$ TeV or $h/\lambda \simeq 56$ for $\Lambda = 10$ TeV, which is feasible. We note that the production of LQs at the LHC depends on the strong coupling constant α_s, and it is nearly independent of the couplings λ_{1i}. In fact, the CMS study took a value of $\lambda_{1i} = 0.3$, which is small enough so that single LQ production can be neglected. In our model, this translates to $h \sim \mathcal{O}(1)$, which is natural. Since the excess is mild, the quoted numbers are very sensitive to further investigation from the collaboration, but it is clear we have a plausible model. We note a small caveat. After electroweak symmetry breaking, the term $\frac{1}{\Lambda_2}h_i' S\bar{L}\chi H$ induces the decay $\chi \to lS$, with a decay width $\Gamma \sim (v_{ew}/\Lambda_2)^2 m_\chi$. This will induce $\tilde{R}_2 \to (l + j + E_{\mathrm{T}})$. However, we see later that dark matter constraints will force us into a benchmark scenario, where we would not expect this scenario to have survived the jet and electron p_T cuts in the CMS $e\nu jj$ study.[4]

IV. DARK MATTER PHENOMENOLOGY

In this section, we discuss the dark matter phenomenology of our model. Since we aim at explaining the LQ excess with a large branching ratio into dark matter in the context of a gauge-invariant theory, we need to necessarily add two fields: a dark matter and a scalar field. There are two possibilities: either one of χ and S can be the dark matter candidate. We first discuss the case of scalar dark matter S and subsequently discuss the bounds on the fermionic candidate χ. The dark matter stability is guaranteed by the discrete symmetry. We note that in the absence of the symmetry, there is no need for the singlet scalar S, and the fermion χ is enough to satisfy the quantum numbers. However, there is a fast decay channel through the $h_i'\bar{L}\chi H$ term in that case.

[3] We note that there are corrections to this mass splitting coming from the dimension-five operators in Eq. (13). However, these corrections will not significantly change our results.

[4] In principle, this signal can also be avoided by choosing Λ_2 large enough that the χ decay happens outside the detector.

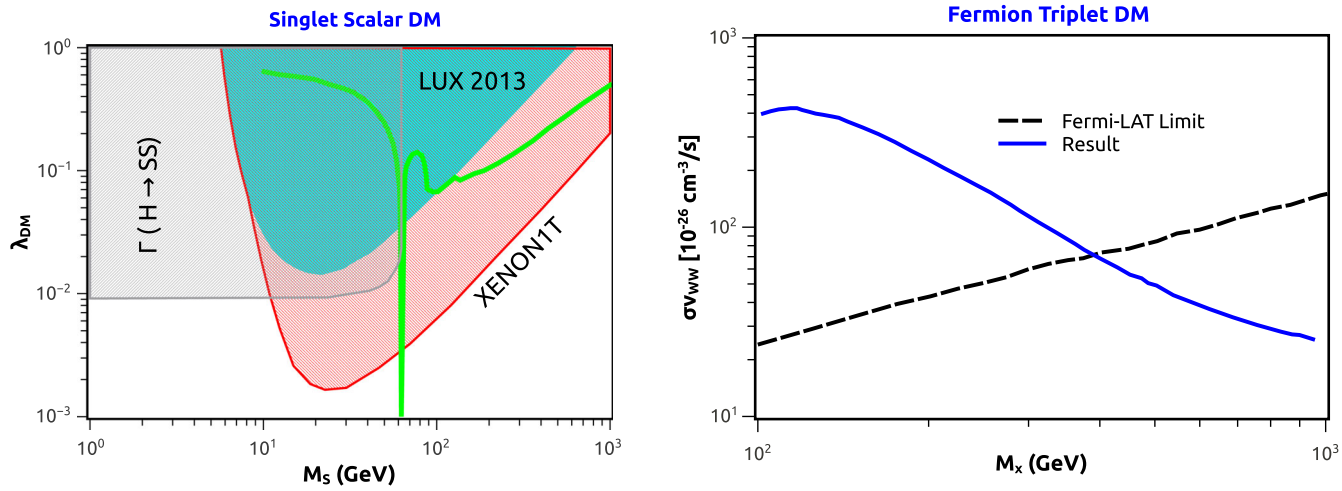

FIG. 4 (color online). *Left*: Direct detection and Higgs width constraints on the singlet scalar dark matter scenario. Current LUX bound excludes masses below ~100 GeV. Projected XENON1T limit will be able to rule out the entire few GeV–1 TeV mass range. *Right:* Annihilation cross section into WW final states for the triplet fermion dark matter model along with the Fermi-LAT dwarf galaxy exclusion limit. We conclude that Fermi-LAT rules out fermion triplet dark matter below ~400 GeV.

A. Scalar dark matter

The scalar S can annihilate through the Higgs portal. Specifically, the relevant terms in the Lagrangian are

$$L \supset \frac{1}{2}\partial_\mu S \partial^\mu S - \frac{m_0^2}{2} S^2 - \frac{\lambda_s}{4} S^4 - \frac{\lambda_{DM}}{4} S^2 H^\dagger H. \tag{20}$$

After electroweak symmetry breaking, shifting the Higgs by its vacuum value $h \to h + v_{ew}$ (where h denotes the physical Higgs), and using $H^\dagger H = \sqrt{2} h v_{ew}$, the S-dependent part of the potential becomes

$$V = \frac{1}{2}\left(m_0^2 + \frac{\lambda_{DM}}{4} v_{ew}^2\right) S^2 + \frac{\lambda_s}{4} S^4 + \frac{\lambda_{DM}}{2\sqrt{2}} v_{ew} S^2 h + \frac{\lambda_{DM}}{2} S^2 h^2. \tag{21}$$

The mass of the dark matter is given by $m_S^2 = m_0^2 + \frac{\lambda_{DM}}{4} v_{ew}^2$. We will assume that the couplings satisfy conditions for the existence of a stable vacuum, and a thermal history for S (typically, this amounts to requiring $\lambda_{DM} \geq 10^{-8}$). The coupling λ_{DM} sets the relic abundance as well as the spin-independent scattering cross section of the dark matter candidate. There are only two free parameters: λ_{DM} and the mass m_S. If S is lighter than half of the Higgs mass, the $h \to SS$ channel becomes kinematically available and changes the measured invisible width of Higgs. The current limit on this is roughly 10%–15% [20,21], and a projected bound of 5% at 14 TeV LHC after 300 fb^{-1} has been claimed [22]. We use the latter. The Higgs branching ratio into S is

$$\mathrm{Br}_{h\to SS} = \frac{\Gamma_{h\to SS}}{\Gamma_{\mathrm{vis}} + \Gamma_{h\to SS}}, \tag{22}$$

where $\Gamma_{\mathrm{vis}} = 4.07$ MeV for $M_h = 125$ GeV, and

$$\Gamma_{h\to SS} = \frac{\lambda_{DM}^2 v_{ew}^2}{8 \cdot 32\pi M_h}\left(1 - \frac{4m_S^2}{M_h^2}\right). \tag{23}$$

This bound is depicted in Fig. 4 (grey shaded region). Our results agree well with Refs. [23,24]. It is clear that λ_{DM} has to be smaller than $\sim 10^{-2}$ to obey the Higgs invisible width limit. The relic abundance and the scattering cross section of the scalar as a function of the two relevant parameters λ_{DM} and the mass m_S has been computed. The relic density is driven by the s-channel annihilation into Standard Model particles. There is a subdominant annihilation into hh, through the quartic scalar interaction $S^2 h^2$ in Eq. (21) and by t-channel S exchange. In Fig. 4 the region determined by the green curve yields the right abundance in agreement with Refs. [23,25]. The cyan region is ruled out by LUX bounds based on the 2013 data [26], whereas the red one is excluded by the projected XENON1T results [27]. Our numerical calculations are performed using MICROMEGAS [28]. Clearly, thermally produced singlets S are excluded by direct detection data for $m_S \lesssim 100$ GeV, unless it is at the Higgs resonance. In order for the LQ to decay to dark matter, we need $m_S \leq 325$ GeV. Thus from Fig. 4 we see that the next run of XENON1T and LUX will decisively rule out this model.

B. Fermionic triplet dark matter

The field χ is a fermionic triplet with a Dirac mass term. Its couplings to the Standard Model relevant for relic density calculations and indirect/direct detection bounds is that of supersymmetric wino dark matter.[5] Triplet dark

[5]Winos are Majorana, whereas χ is Dirac. However, for the purposes of indirect/direct bounds in this case, the results are similar.

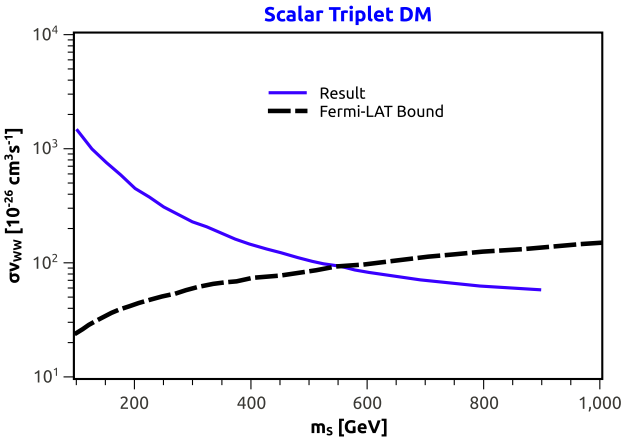

FIG. 5 (color online). The viable and excluded mass range of the scalar triplet model. The blue line is the annihilation cross section to WW final state in the current Universe. The black line is the bound from Fermi-LAT data.

matter is under severe tension in the mass range we are considering (the case of the wino has been studied in detail [29]). We outline the main bounds here. For the triplet fermionic dark matter $(\chi^0, \chi^\pm)$, the relevant portion of the interaction Lagrangian with the Standard Model comes through gauge interactions:

$$\mathcal{L}_{\rm int} = -\frac{e}{s_W}(\bar{\tilde{\chi}}^0\gamma^\mu\tilde{\chi}^- W_\mu^\dagger + \text{H.c.}) + e\frac{c_W}{s_W}\overline{\tilde{\chi}^-}\gamma^\mu\tilde{\chi}^- Z_\mu + e\overline{\tilde{\chi}^-}\gamma^\mu\tilde{\chi}^- A_\mu. \quad (24)$$

Here, e is the electric charge, $s_W = \sin\theta_W$ and $c_W = \cos\theta_W$, with θ_W being the Weinberg angle. The leading contribution to the χ-quark interaction comes from one-loop interactions. After evaluating the relevant diagrams, it turns out that

$$\sigma^{SI} \sim 10^{-47}\ \text{cm}^2 \quad (25)$$

in the mass range of interest. We refer to [30] for further details. This may be probed by XENON1T. On the other hand, the model is severely constrained by indirect detection data. Continuum photons arise from the tree-level annihilation process $\chi^0\chi^0 \to W^+W^-$. Fermi-LAT dwarf galaxy data [31] rule out triplet dark matter masses up to around 400 GeV, while galactic center data rules it out up to around 700 GeV for either NFW or Einasto profiles [32]. Such bounds become stronger (weaker) if one considers steeper (core) profiles. For instance, the current limits from using dwarf spheroidal data and the PASS-8 software from Fermi-LAT Collaboration rule out the canonical WIMP for masses below ~100 GeV. Albeit, recent discoveries of optical signatures of black holes in dwarf galaxies indicate that low-mass galaxies can indeed host intermediate massive black holes. If one includes intermediate massive black holes in dwarf galaxies still without spoiling the measured velocity dispersion of the stars, the constraints on the dark matter annihilation cross section may become orders of magnitude stronger [33], ruling out thermal wino-DM masses up to 1 TeV.

C. Variations and other options for dark matter

In this subsection, we briefly discuss other dark matter possibilities and variations of the model we described. We will only consider dark sectors with $Y = 0$. Candidates with $Y \neq 0$ have vectorlike interactions with the Z boson that give spin-independent scattering cross sections which are ruled out by current direct detection constraints. This conclusion could be altered if, for example, χ dark matter is Majorana, in which case it cannot have a vectorlike coupling to Z. This is reminiscent of Higgsino dark matter in supersymmetry. However, such a mass term would violate lepton number in our case and would have to be generated at a high scale, as mentioned before. We are, thus, led to the variations outlined in this section.

1. Fermion singlet dark matter

A simple variation of the model presented before is

$$\tilde{R}_2 = (3, 2, 1/6)_+$$
$$\chi = (1, 1, 0)_- \quad (26)$$
$$S = (1, 1, 0)_-, \quad (27)$$

with a Lagrangian still given by Eq. (13). As we have mentioned before, it is possible in this variation to accommodate a gauge singlet Dirac fermion dark matter if χ is lighter than S. The dark matter annihilation and scattering cross sections are set by the fermionic dark matter Higgs portal.[6] This has been studied in detail by [35]. In this context the coupling between χ and H can be written as

$$L \supset \frac{1}{\Lambda}(v_{ew}h + (1/2)h^2)(\cos\xi\bar{\chi}\chi + \sin\xi\bar{\chi}i\gamma_5\chi), \quad (28)$$

where $\cos\xi$ and $\sin\xi$ control the relative strengths of the CP-conserving and -violating terms. Similar to the scalar Higgs portal, direct detection experiments severely constrain this model. Current LUX bounds can accommodate $m_\chi \sim 300$ GeV for $\cos\xi^2 \sim 0.5$. However, for smaller dark matter masses, the pseudoscalar component must dominate rapidly to evade bounds. This is an unnatural tuning of the

[6]The Z_2 symmetry forbids a term like $\bar{\chi}\chi S$. Such a term could have been allowed if only χ was odd under the Z_2 symmetry, while S was even. In that case, a term like $SH^\dagger H$, allowed by the symmetries, would have mixed S with the Higgs, allowing for a Higgs portal connection for χ through the $\bar{\chi}\chi S$ term. Such models have been studied by [34]. In our case, this charge assignment under Z_2 would forbid the all-important $\frac{1}{\Lambda_1}h_i S\chi\bar{Q}\tilde{R}_2$ term.

Lagrangian. The resonant Higgs portal with $m_\chi \sim 60$ GeV is allowed for all values of $\cos\xi$. However, this is a very specific dark matter mass that is not a priori motivated from UV physics. In the next section we discuss another possible variation of the dark sector.

2. Scalar triplet dark matter

Another variation of the original model that may be considered is to switch the $SU(2)$ charges of the scalar and fermion, leading to the following particle content,

$$\tilde{R}_2 = (3, 2, 1/6)_+$$
$$\chi = (1, 1, 0)_- \tag{29}$$
$$S = (1, 3, 0)_-, \tag{30}$$

with the same Lagrangian in Eq. (13) as before. A quartic interaction with the Higgs is also possible, which will induce mass splitting within the multiplet. When the interaction strength is small, the splitting reverts to the usual 166 MeV induced by gauge couplings. The constraints from indirect detection are very stringent in the mass range we are considering [36], as one can see in Fig. 5, where we display the annihilation cross section of scalar triplets into WW final states and the Fermi bound. It is evident that Fermi dwarf galaxy data rules out scalar triplet dark matter up to ~550 GeV.

D. Comments on collider signatures

In the previous sections, we have described the dark matter candidates that are capable of coupling to LQs and satisfying all constraints from colliders, proton decay, and direct and indirect detection experiments. The possible candidates are quite limited:

(1) A scalar singlet in the mass range of 100–325 GeV, coupled to the Higgs portal, evades LUX bounds;
(2) A fermion singlet in the mass range of 300 GeV with a significant pseudoscalar coupling;
(3) A scalar or fermionic singlet in the resonant Higgs portal, with mass ~60–65 GeV.

Scalar and fermionic triplets, which are the other possibilities, are ruled out by indirect detection in the mass range of interest. We now briefly discuss the opportunities for collider studies of the scenarios above. After the LQ with mass ~650 GeV decays to χ and S, there is a further decay of χ to a lepton and S. Thus, the final state from each LQ decay consists of l, j and $E_{\rm T}$. It would be very interesting to probe this scenario in $2l + 2j + E_{\rm T}$ events. For dark matter in the mass range 100–325 GeV that we are considering in scenarios 1 and 2, the lepton and jets are expected to be significantly softer than the cuts employed in the LQ $e\nu jj$ study. Moreover, since $m_{LQ} \sim m_S + m_\chi$, this is a compressed scenario where the missing energy release is small. It would be very interesting to probe this scenario in events with significant boosting due to the presence of high p_T initial jets [37], where appreciable $E_{\rm T}$ to distinguish signal and background may be obtained.

V. CONCLUSIONS

This paper has been motivated by the mild excess seen by CMS in the $eejj$ and $e\nu jj$ channels, in its first-generation LQ search. If the excess is indeed due to a LQ in the mass range of 550–650 GeV, then there has to be branching to other states which are not captured in those channels. Given the stringent bounds on second- and third-generation LQs, the idea of tying LQs to dark matter is well motivated.

Among the leptoquark models presented in Table II, we were left with only R_2 and $\tilde{R}_2$ to avoid fast proton decay since the quantum number $\tilde{R}_2$ seems more attractive from a model-building perspective. Taking $\tilde{R}_2$ as our candidate, the gauge charges of the LQ, stability of the dark matter, and avoiding the large Z-mediated nucleon-dark matter scattering cross section force us to consider a limited set gauge charge assignments in the dark sector. The dark matter can be either a scalar/fermion triplet or a scalar/fermion singlet. The former cases are ruled out by Fermi-LAT data in the mass range of interest. For the singlets, the following options emerge:

(1) A scalar singlet in the mass range of 100–325 GeV, coupled to the Higgs portal;
(2) A fermion singlet in the mass range of 300 GeV with a significant pseudoscalar coupling to the Higgs portal;
(3) A scalar or fermionic singlet in the resonant Higgs portal, with mass ~60–65 GeV.

Those finding are consistent with muon magnetic moment, proton decay, and K^0 and B^0 meson constraints. Finally, we have also outlined collider strategies for exploring these cases. The most promising search channels would be $2l + 2j + E_{\rm T}$ events, with significant boosting due to the compressed nature of the spectrum.

ACKNOWLEDGEMENTS

The authors are indebted to Josh Berger for clarifying the results and Eugenio Del Nobile for important discussions concerning the muon magnetic moment. F. Q. is partly supported by the U.S. Department of Energy Award No. SC0010107 and the Brazilian National Counsel for Technological and Scientific Development (CNPq). K. S. is supported by NASA Astrophysics Theory Grant No. NNH12ZDA001N. A. S. is supported by ESF Grant No. MTT8, by the SF0690030s09 project and by the European Programme No. PITN-GA-2009-237920 (UNILHC).

[1] J. C. Pati and A. Salam, Phys. Rev. D **10**, 275 (1974); **11**, 703(E) (1975).
[2] H. Georgi and S. L. Glashow, Phys. Rev. Lett. **32**, 438 (1974).
[3] E. Farhi and L. Susskind, Phys. Rep. **74**, 277 (1981); S. Dimopoulos and L. Susskind, Nucl. Phys. **B155**, 237 (1979).
[4] J. L. Hewett and T. G. Rizzo, Phys. Rev. D **56**, 5709 (1997).
[5] M. Leurer, Phys. Rev. D **49**, 333 (1994).
[6] S. Davidson, D. C. Bailey, and B. A. Campbell, Z. Phys. C **61**, 613 (1994).
[7] S. S. Gershtein, A. A. Likhoded, and A. I. Onishchenko, Phys. Rep. **320**, 159 (1999); I. Dorsner and P. Fileviez Perez, Nucl. Phys. **B723**, 53 (2005); B. Gripaios, J. High Energy Phys. 02 (2010) 045; P. Fileviez Perez, T. Han, T. Li, and M. J. Ramsey-Musolf, Nucl. Phys. **B819**, 139 (2009); D. Aristizabal Sierra, M. Hirsch, and S. G. Kovalenko, Phys. Rev. D **77**, 055011 (2008); P. Y. Popov, A. V. Povarov, and A. D. Smirnov, Mod. Phys. Lett. A **20**, 3003 (2005); K. S. Babu and J. Julio, Nucl. Phys. **B841**, 130 (2010).
[8] CMS Collaboration, Report No. PAS EXO-12-042, https://cds.cern.ch/record/1542374/files/.
[9] G. Aad *et al.* (ATLAS Collaboration), Eur. Phys. J. C **72**, 2151 (2012).
[10] V. Khachatryan *et al.* (CMS Collaboration), Phys. Lett. B **739**, 229 (2014).
[11] Report No. PAS EXO13010, https://twiki.cern.ch/twiki/bin/genpdf/CMSPublic/.
[12] CMS Collaboration, Report No. PAS EXO-12-041, http://cds.cern.ch/record/1742179/files/.
[13] Y. Bai and J. Berger, arXiv:1407.4466.
[14] W. Buchmuller, R. Ruckl, and D. Wyler, Phys. Lett. B **191**, 442 (1987); **448**, 320(E) (1999).
[15] A. J. Davies and X. G. He, Phys. Rev. D **43**, 225 (1991).
[16] J. M. Arnold, B. Fornal, and M. B. Wise, Phys. Rev. D **88**, 035009 (2013).
[17] F. S. Queiroz and W. Shepherd, Phys. Rev. D **89**, 095024 (2014); R. M. Carey, K. R. Lynch, J. P. Miller, B. L. Roberts, W. M. Morse, Y. K. Semertzides, V. P. Druzhinin, B. I. Khazin *et al.*, Report No. FERMILAB-PROPOSAL-0989; A. S. Kronfeld *et al.*, arXiv:1306.5009.
[18] J. P. Saha, B. Misra, A. Kundu, Phys. Rev. D **81**, 095011 (2010).
[19] M. Cirelli and A. Strumia, New J. Phys. **11**, 105005 (2009).
[20] G. Belanger, B. Dumont, U. Ellwanger, J. F. Gunion, and S. Kraml, Phys. Rev. D **88**, 075008 (2013).
[21] J. Ellis and T. You, J. High Energy Phys. 06 (2013) 103.
[22] M. E. Peskin, arXiv:1207.2516.
[23] A. De Simone, G. F. Giudice, and A. Strumia, J. High Energy Phys. 06 (2014) 081.
[24] M. Farina, D. Pappadopulo, and A. Strumia, J. High Energy Phys. 08 (2013) 022.
[25] F. S. Queiroz and K. Sinha, Phys. Lett. B **735**, 69 (2014); J. M. Cline, K. Kainulainen, P. Scott, and C. Weniger, Phys. Rev. D **88**, 055025 (2013).
[26] D. S. Akerib *et al.* (LUX Collaboration), Phys. Rev. Lett. **112**, 091303 (2014).
[27] P. Cushman, C. Galbiati, D. N. McKinsey, H. Robertson, T. M. P. Tait, D. Bauer, A. Borgland, B. Cabrera *et al.*, arXiv:1310.8327.
[28] G. Belanger, F. Boudjema, A. Pukhov, and A. Semenov, Comput. Phys. Commun. **185**, 960 (2014); G. Belanger, F. Boudjema, P. Brun, A. Pukhov, S. Rosier-Lees, P. Salati, and A. Semenov, Comput. Phys. Commun. **182**, 842 (2011).
[29] J. Fan and M. Reece, J. High Energy Phys. 10 (2013) 124; R. Easther, R. Galvez, O. Ozsoy, and S. Watson, Phys. Rev. D **89**, 023522 (2014); T. Cohen, M. Lisanti, A. Pierce, and T. R. Slatyer, J. Cosmol. Astropart. Phys. 10 (2013) 061; R. Allahverdi, B. Dutta, and K. Sinha, Phys. Rev. D **86**, 095016 (2012); B. Dutta, T. Kamon, N. Kolev, K. Sinha, K. Wang, and S. Wu, Phys. Rev. D **87**, 095007 (2013); A. Djouadi, A. Falkowski, Y. Mambrini, and J. Quevillon, Eur. Phys. J. C **73**, 2455 (2013).
[30] J. Hisano, K. Ishiwata, and N. Nagata, Phys. Lett. B **690**, 311 (2010).
[31] M. Ackermann *et al.*, Phys. Rev. D **86**, 022002 (2012).
[32] A. Hryczuk, I. Cholis, R. Iengo, M. Tavakoli, and P. Ullio, J. Cosmol. Astropart. Phys. 07 (2014) 031.
[33] A. X. Gonzalez-Morales, S. Profumo, and F. S. Queiroz, Phys. Rev. D **90**, 103508 (2014).
[34] S. Esch, M. Klasen, and C. E. Yaguna, Phys. Rev. D **88**, 075017 (2013).
[35] M. A. Fedderke, J. Y. Chen, E. W. Kolb, and L. T. Wang, J. High Energy Phys. 08 (2014) 122.
[36] M. Cirelli, N. Fornengo, and A. Strumia, Nucl. Phys. **B753**, 178 (2006); M. Cirelli, A. Strumia, and M. Tamburini, Nucl. Phys. **B787**, 152 (2007); F. X. Josse-Michaux and E. Molinaro, Phys. Rev. D **87**, 036007 (2013); O. Fischer and J. J. van der Bij, J. Cosmol. Astropart. Phys. 01 (2014) 032.
[37] B. Dutta, A. Gurrola, W. Johns, T. Kamon, P. Sheldon, and K. Sinha, Phys. Rev. D **87**, 035029 (2013); A. G. Delannoy, B. Dutta, A. Gurrola, W. Johns, T. Kamon, E. Luiggi, A. Melo, P. Sheldon, K. Sinha, K. Wang, and S. Wu, Phys. Rev. Lett. **111**, 061801 (2013); B. Dutta, W. Flanagan, A. Gurrola, W. Johns, T. Kamon, P. Sheldon, K. Sinha, K. Wang, and S. Wu, Phys. Rev. D **90**, 095022 (2014).